Available online at www.sciencedirect.com
ScienceDirect
International Journal of Non-Linear Mechanics 43 (2008) 264–276
INTERNATIONAL JOURNAL OF NON-LINEAR MECHANICS
www.elsevier.com/locate/nlm

Mechanics of polymeric membranes subjected to chemical exposure

A.P.S. Selvadurai*, Q. Yu[1]

Department of Civil Engineering and Applied Mechanics, McGill University, 817 Sherbrooke Street West, Montréal, Que., Canada H3A 2K6

Received 4 January 2007; received in revised form 3 November 2007; accepted 11 December 2007

Dedicated to the memory of Professor R.S. Rivlin (1915–2005)

Abstract

The mechanics of polymeric hyperelastic membranes that are subjected to uniform transverse pressure loading are discussed. The paper also focuses on the membrane behaviour when there is loss of hyperelasticity resulting from the removal of plasticizer from the polymeric material as a result of chemical exposure. Constitutive models presented describe the influence of both hyperelasticity and rate-sensitivity on the mechanical behaviour of the polymeric membrane in its natural and chemically exposed states. The constitutive models developed through experimental investigations are implemented in computational techniques to develop solutions to the membrane deformation problems.

Keywords: Polymeric membranes; Hyperelasticity; Chemical exposure; Rate-dependent constitutive models; Membrane deformations; Finite element modelling

1. Introduction

Polymeric membranes are used extensively as components of geo-environmental barrier systems that are used to prevent the migration of contaminants and hazardous wastes. A characteristic feature of polymeric membranes is their hyperelasticity, which is a beneficial attribute particularly in situations where the engineered membrane barrier can experience large deformational behaviour during ground movement. The hyperelasticity and the accompanying rate-dependency of polymeric membranes is a result of plasticizers that are introduced into the material during its manufacture; its depletion, particularly due to leaching by chemicals, can result in the *embrittlement* of the polymeric membrane. Fig. 1 illustrates the progressive time-dependent embrittlement of a PVC membrane material during exposure to pure ethanol. The loss of hyperelasticity during chemical action is a cause for environmental concern, particularly because geo-synthetic membranes are used extensively for perpetual geo-environmental containment, without due attention being paid to the issue of loss of hyperelasticity due to embrittlement. This paper develops a constitutive theory that can describe the hyperelastic behaviour of the rate-sensitive polymeric membrane material in its intact condition and examines the changes that account for the loss of hyperelasticity and embrittlement during exposure to chemicals such as ethanol. The constitutive theories, developed and validated by appeal to experimentation, are implemented in a research-category computer code to examine the mechanics of edge-supported circular membranes both in their intact and chemically exposed conditions. Both axisymmetric and off-axis indentations of polymeric membranes have been used to validate the constitutive models. In this paper, the computational procedures are applied to examine the mechanics of square and triangular edge-supported membranes that are subjected to uniform pressure. Further applications include the fluid pressure loading of a membrane, where a circular patch of the membrane experiences embrittlement due to the leaching of the plasticizer by chemical exposure. The stress analysis of the problems is performed by implementing the relevant constitutive models in the ABAQUS finite element code.

2. Constitutive modelling

Modern mechanics of hyperelastic materials can be traced to the seminal studies of Rivlin, which are documented in his

* William Scott Professor and James McGill Professor. Corresponding author. Tel.: +1 514 398 6672; fax: +1 514 398 7361.
E-mail addresses: patrick.selvadurai@mcgill.ca (A.P.S. Selvadurai), Qifeng.Yu2@boeing.com (Q. Yu).
[1] Currently at Boeing Canada Technology, Winnipeg Division, 99 Murray Park Road, Winnipeg, Man., Canada R3J 3M6.

0020-7462/$ - see front matter © 2007 Elsevier Ltd. All rights reserved.
doi:10.1016/j.ijnonlinmec.2007.12.004

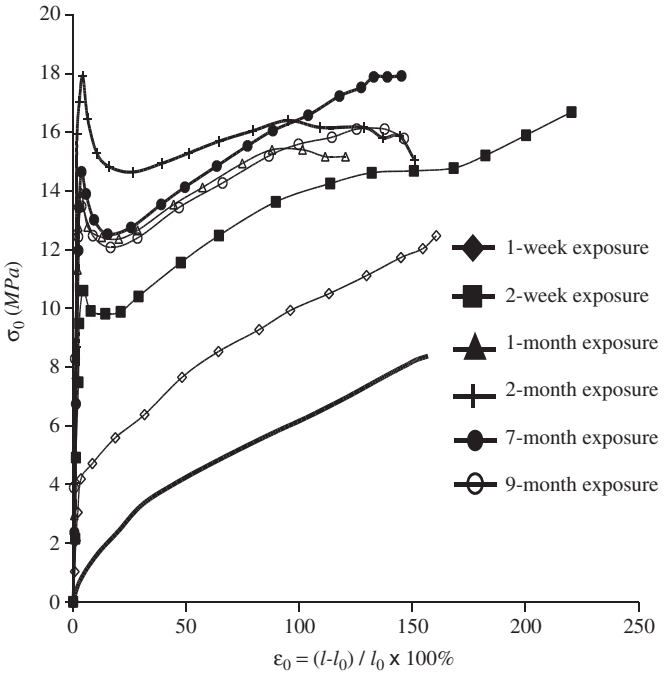

Fig. 1. Uniaxial stress–strain behaviour of a PVC membrane material subjected to chemical (ethanol) exposure.

collected works edited by Barenblatt and Joseph [1]. The majority of research in the area is applicable to pure rubber-like hyperelastic materials, which have imperceptible irreversible phenomena in terms of non-coincidence of loading and unloading paths, resulting in both energy dissipation during cycles of loading and the development of irreversible deformations upon removal of loads. The constitutive potentials associated with rubber-like hyperelastic materials including those attributed to Mooney–Rivlin, neo-Hookean, Blatz–Ko, Yeoh, Ogden, Gent and others are well documented in classical literature in finite elasticity [2–5]. Reviews and extensive discussions of the range of constitutive models that have been proposed to describe hyperelastic responses of rubber-like materials can be found in the articles by Deam and Edwards [6], Ogden [7], Lur'e [8], Drozdov [9], Dorfmann and Muhr [10], Boyce and Arruda [11], Fu and Ogden [12], Besdo et al. [13], Busfield and Muhr [14], Saccomandi and Ogden [15], Selvadurai [16] and Rivlin [17]. In addition, the adequacy of the Mooney–Rivlin form of a strain energy function for examining transverse deflections of rubber membranes that experience moderately large strains was recently documented by Selvadurai [18].

In contrast, glassy polymeric materials, such as PVC, exhibit appreciable irreversible effects that include the development of permanent strains during loading–unloading cycles and strain rate effects [19,20]. The modelling of materials that exhibit irreversible, path-dependent, rate-sensitive effects has been the subject of much research, both past and recent, and examples of the development of constitutive models are given by Boyce and Arruda [11], Arruda et al. [19], Sweeney and Ward [20], Boyce et al. [21], Wineman and Rajagopal [22], Rajagopal and Wineman [23], Bergström and Boyce [24], Septanika and Ernst [25,26], Makradi et al. [27], Amin et al. [28], Gurtin and Anand [29] and Selvadurai and Yu [30]. Also of interest are recent studies by Shaw et al. [31] that examine the chemorheological behaviour of elastomers at elevated temperatures. In this paper we adopt and extend the model proposed by Boyce et al. [21] to develop plausible constitutive models for the PVC material in both its intact and chemically exposed states. A fundamental assumption in the modelling is that the path-dependency and irreversibility associated with the mechanics of the PVC material can be captured by a model that is used to describe the hyperelastic behaviour of an elastic material with added constraints to account for the rate-sensitivity and path-dependency effects. Other examples along these lines are the studies by Ogden and Roxburgh [32,33] that use the concept of an internal variable, associated with deformation-related damage development to provide a rational explanation of the Mullins effect observed in the mechanical behaviour of certain types of hyperelastic rubber-like materials (see also [34,35]).

The visco-plastic constitutive model for PVC proposed in this paper considers large strain elasticity phenomena, irreversible deformation and strain rate effects. The results of experiments conducted for constitutive model development were presented by Yu and Selvadurai [36] and the associated constitutive model development was discussed in greater detail by Selvadurai and Yu [30]. Studies presented in [30] and [36] suggest that PVC materials can undergo strains moderately large enough to render an approach based on an incremental rate-dependent theory of material behaviour of limited value. Therefore, we formulate a constitutive model that accounts for finite deformations of the PVC material. The position of a generic particle in the reference configuration is denoted by the Cartesian coordinates X_A $(A=1, 2, 3)$ and its position in the deformed configuration is denoted by x_i $(i=1, 2, 3)$. The deformation gradient tensor is given by

$$\mathbf{F} = \frac{\partial x_i}{\partial X_A}. \tag{2.1}$$

We restrict attention to PVC materials that are largely incompressible, which requires that $\det \mathbf{F} = 1$. Following the approaches proposed by Kröner [37] and Lee [38] to describe the mechanics of continua undergoing finite deformations that exhibit both reversible and irreversible components (see also [29,39–43]), we assume that the total deformation gradient tensor $\mathbf{F}$ admits a *product decomposition* into its elastic (e) and irreversible (u) components, i.e.

$$\mathbf{F} = \mathbf{F}^{\mathrm{e}}\mathbf{F}^{\mathrm{u}}. \tag{2.2}$$

The strain tensors associated with the elastic and irreversible deformations are defined by $\mathbf{B}^{\mathrm{e}}$ and $\mathbf{B}^{\mathrm{u}}$, respectively, where

$$\mathbf{B}^{\mathrm{e}} = \mathbf{F}^{\mathrm{e}}(\mathbf{F}^{\mathrm{e}})^{\mathrm{T}}, \quad \mathbf{B}^{\mathrm{u}} = \mathbf{F}^{\mathrm{u}}(\mathbf{F}^{\mathrm{u}})^{\mathrm{T}} \tag{2.3}$$

and the strain rates are defined by [44,45]

$$\mathbf{L} = \dot{\mathbf{F}}\mathbf{F}^{-1} = \mathbf{D} + \mathbf{W} = \dot{\mathbf{F}}^{\mathrm{e}}(\mathbf{F}^{\mathrm{e}})^{-1} + \mathbf{F}^{\mathrm{e}}[\dot{\mathbf{F}}^{\mathrm{u}}(\mathbf{F}^{\mathrm{u}})^{-1}](\mathbf{F}^{\mathrm{e}})^{-1},$$

$$\mathbf{L}^{\mathrm{u}} = \dot{\mathbf{F}}^{\mathrm{u}}(\mathbf{F}^{\mathrm{u}})^{-1}, \quad \mathbf{D}^{\mathrm{u}} = \tfrac{1}{2}[\mathbf{L}^{\mathrm{u}} + (\mathbf{L}^{\mathrm{u}})^{\mathrm{T}}]. \tag{2.4}$$

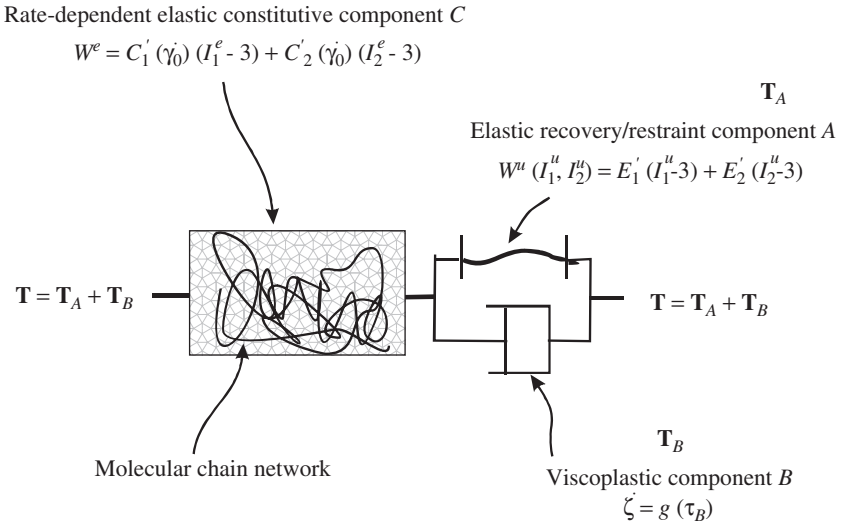

Fig. 2. Schematic representation of the constitutive components.

The invariants of $\mathbf{B}^{\mathrm{e}}$ and $\mathbf{B}^{\mathrm{u}}$ are

$$I_1^h = (\lambda_1^h)^2 + (\lambda_2^h)^2 + (\lambda_3^h)^2, \quad I_2^h = \frac{1}{(\lambda_1^h)^2} + \frac{1}{(\lambda_2^h)^2} + \frac{1}{(\lambda_3^h)^2},$$

$$I_3^h = \lambda_1^h \lambda_2^h \lambda_3^h = 1, \quad (h = \mathrm{e}, \mathrm{u}) \tag{2.5}$$

and λ_i^{e} and λ_i^{u} $(i = 1, 2, 3)$ are, respectively, the principal stretches of the elastic and irreversible components. The general form of the constitutive model for the PVC material has been selected to conform to a generic version with components as shown in Fig. 2.

2.1. A constitutive model for the untreated PVC

The calibration of experimental results [30,36] with a wider class of strain energy functions indicates that for *moderately large strains*, the constitutive behaviour of the PVC material can be adequately characterized by choosing an internal energy function with a mathematical form similar to the Mooney–Rivlin type [18,46–48]. Thus, component C of the model shown in Fig. 2 is represented by a pseudo-elastic behaviour with an internal energy function of the Mooney–Rivlin type. We also note that it is sufficient to characterize the constitutive behaviour of the PVC material during *monotonic loading* without *unloading*. In this case, there are no irreversible effects and the total deformation gradient $\mathbf{F}$ can be interpreted as an elastic deformation gradient $\mathbf{F}^{\mathrm{e}}$. The stress $\mathbf{T}_{\mathrm{C}}$ associated with the model C, which is the total Cauchy stress $\mathbf{T}$ in the material, is assumed to be an isotropic function of the elastic strain tensor $\mathbf{B}^{\mathrm{e}}$ and takes the form

$$\mathbf{T} = \mathbf{T}_{\mathrm{C}} = -\tilde{p}^{\mathrm{e}}\mathbf{I} + \psi_1^{\mathrm{e}}\mathbf{B}^{\mathrm{e}} + \psi_2^{\mathrm{e}}(\mathbf{B}^{\mathrm{e}})^2,$$
$$\psi_1^{\mathrm{e}} = 2\left(\frac{\partial W^{\mathrm{e}}}{\partial I_1^{\mathrm{e}}} + I_1^{\mathrm{e}}\frac{\partial W^{\mathrm{e}}}{\partial I_2^{\mathrm{e}}}\right), \quad \psi_2^{\mathrm{e}} = -2\frac{\partial W^{\mathrm{e}}}{\partial I_2^{\mathrm{e}}}, \tag{2.6}$$

where $\tilde{p}^{\mathrm{e}}$ is a scalar pressure. Considering the approach proposed by Sweeney and Ward [20] to account for the influence of the strain rate effects on the strain energy function, we adopt the following form of internal energy function for the PVC material:

$$W^{\mathrm{e}}(I_1^{\mathrm{e}}, I_2^{\mathrm{e}}) = C_1'(I_1^{\mathrm{e}} - 3) + C_2'(I_2^{\mathrm{e}} - 3), \tag{2.7}$$

where

$$C_1' = C_1 + \begin{cases} \kappa_1 \ln(|\dot{\gamma}_0|/\dot{\gamma}_c) & (|\dot{\gamma}_0| \geqslant \dot{\gamma}_c), \\ 0 & (|\dot{\gamma}_0| < \dot{\gamma}_c), \end{cases}$$

$$C_2' = C_2 + \begin{cases} \kappa_2 \ln(|\dot{\gamma}_0|/\dot{\gamma}_c) & (|\dot{\gamma}_0| \geqslant \dot{\gamma}_c), \\ 0 & (|\dot{\gamma}_0| < \dot{\gamma}_c). \end{cases} \tag{2.8}$$

The thermodynamic basis for introducing the dependency of W^{e} on $\dot{\gamma}_0$ is discussed in Selvadurai and Yu [30]. In (2.8), $\dot{\gamma}_0$ is a generalized form of a combined stretch rate that depends only on the principal stretches $\bar{\lambda}_i$ $(i = 1, 2, 3)$, such that

$$\dot{\gamma}_0 = \frac{\mathrm{d}\gamma_0}{\mathrm{d}t}, \quad \gamma_0 = [(\bar{\lambda}_1 - 1)^{1/\alpha} + (\bar{\lambda}_2 - 1)^{1/\alpha} + (\bar{\lambda}_3 - 1)^{1/\alpha}]^{\alpha}, \tag{2.9}$$

where $\bar{\lambda}_i$ $(i = 1, 2, 3)$ have a *conditional dependence* on the total principal stretches λ_i to take into consideration either the *stretching* or the *unloading* response, i.e.

$$\bar{\lambda}_i = \begin{cases} \lambda_i & (\lambda_i \geqslant 1) \quad i = (1, 2, 3), \\ 1 & (\lambda_i < 1) \quad i = (1, 2, 3) \end{cases} \tag{2.10}$$

and α is a material parameter that accounts for combined stretch. We note that when a specimen is subjected to a uniaxial stretch, the principal stretches in the lateral directions are less than unity and therefore the definition of γ_0 reduces to that of the uniaxial strain ε_0. In (2.8), C_1' and C_2' are the modified Mooney–Rivlin-type parameters; κ_1 and κ_2 are parameters that define the strain rate sensitivity and $\dot{\gamma}_c$ is defined as the *rate-independent*

threshold strain rate, i.e. a parameter that controls the manifestation of strain rate effects. At loading rates $|\dot{\gamma}_0| \leqslant \dot{\gamma}_c$, the strain rate effects are disregarded. The loading behaviour was examined by considering the uniaxial response of a specimen of PVC tested up to failure at loading rates $\dot{\varepsilon}_0 = 0.4$, and 40%/min. The material parameters required to define C_1' and C_2' were developed using experimental data and the specific values determined were as follows:

$$C_1 \approx 0.23\,\text{MPa}; \quad C_2 \approx 0.53\,\text{MPa}; \quad \kappa_1 = \kappa_2 = \kappa \approx 0.13; \quad \dot{\gamma}_c \approx 5.67 \times 10^{-7}\,\text{s}^{-1}.$$

PVC materials invariably exhibit permanent strains at *any* level of applied strain. Therefore, a visco-plastic model, characterized by an elastic recovery component A in parallel with a visco-plastic component B should be incorporated in series with the component C. Since the component A accounts for elastic unloading at moderately large strains, we can conclude that the model, which accounts for the unloading response, can also be described by an internal energy function of the Mooney–Rivlin form, i.e.

$$\mathbf{T}_A = -\tilde{p}^{\mathrm{u}}\mathbf{I} + \psi_1^{\mathrm{u}}\mathbf{B}^{\mathrm{u}} + \psi_2^{\mathrm{u}}(\mathbf{B}^{\mathrm{u}})^2,$$

$$\psi_1^{\mathrm{u}} = 2\left(\frac{\partial W^{\mathrm{u}}}{\partial I_1^{\mathrm{u}}} + I_1^{\mathrm{u}}\frac{\partial W^{\mathrm{u}}}{\partial I_2^{\mathrm{u}}}\right), \quad \psi_2^{\mathrm{u}} = -2\frac{\partial W^{\mathrm{u}}}{\partial I_2^{\mathrm{u}}}, \tag{2.11}$$

where $\tilde{p}^{\mathrm{u}}$ is a scalar pressure and

$$W^{\mathrm{u}}(I_1^{\mathrm{u}}, I_2^{\mathrm{u}}) = E_1'(I_1^{\mathrm{u}} - 3) + E_2'(I_2^{\mathrm{u}} - 3) \tag{2.12}$$

with the superscript 'u' signifying the unloading mode. In (2.12), we apply a conditional constraint to E_1', i.e.

$$E_1' = \begin{cases} \to \infty & (\dot{\gamma}_0 \geqslant -\dot{\gamma}_c^v), \\ 0 & (\dot{\gamma}_0 < -\dot{\gamma}_c^v) \end{cases} \tag{2.13}$$

and E_2' is treated as a constant. The strain rate-dependent E_1' in (2.13) takes into account the asymmetric behaviour of the elastic recovery component A during a loading–unloading response. The stress $\mathbf{T}_B$ in the component B is defined in terms of the finite plastic strain rate $\mathbf{D}^{\mathrm{u}}$, which is assumed to be related to the deviatoric component of the normalized effective stress tensor $\mathbf{N}_B$. Considering the component B, the visco-plastic effects are modelled through a relationship of the form (see e.g. [49,29])

$$\mathbf{D}^{\mathrm{u}} = \dot{\zeta}\mathbf{N}_B, \quad \mathbf{N}_B = \frac{3}{2\tau_B}\mathbf{T}_B', \quad \tau_B = \left\{\frac{3}{2}\mathrm{tr}[(\mathbf{T}_B')^2]\right\}^{1/2} \tag{2.14}$$

and $\mathbf{T}_B'$ is the deviatoric component of the Cauchy stress tensor $\mathbf{T}_B$ applicable to visco-plastic phenomena, as depicted in Fig. 2. Also, in (2.14) the visco-plastic strain rate $\dot{\zeta}$ is considered to be a function of the effective stress τ_B and the strain rate $\dot{\gamma}_0$, i.e.

$$\dot{\zeta} = \left(\frac{\tau_B}{q}\right)^{1-s}|\dot{\gamma}_0| \begin{cases} \dfrac{1}{(|\dot{\gamma}_0|/\gamma_c^v)^s} & (|\dot{\gamma}_0| \geqslant \dot{\gamma}_c^v), \\ 1 & (|\dot{\gamma}_0| < \dot{\gamma}_c^v). \end{cases} \tag{2.15}$$

In (2.15), s is the *viscous sensitivity* to the strain rate effect. At extremely low loading rates $|\dot{\gamma}_0| \leqslant \dot{\gamma}_c^v$, and the dependency of $\dot{\zeta}$ on the strain rate $\dot{\gamma}_0$ is neglected; therefore, the parameter q can be interpreted as the *static yielding stress* of the material. We note that when $s \approx 0$, the value of $\dot{\gamma}_c^v$ is inapplicable, and the response of the material reduces to that of a purely plastic material.

During a loading stage ($\dot{\gamma}_0 \geqslant 0$) and at extremely low loading rates ($|\dot{\gamma}_0| \leqslant \dot{\gamma}_c^v$), the visco-plastic deformation applicable to the components A and B is constrained by the choice of an infinite value for E_1', with the result that only the elastic deformation of component C is applicable to the PVC material. Upon unloading, however, the visco-plastic deformation is fully activated due to the zero value of E_1' chosen in (2.13). All three components A–C take effect during the unloading of the PVC material. Following Boyce et al. [21], the stress states in the elastic recovery response A (denoted by $\mathbf{T}_A$) and the visco-plastic response B (denoted by $\mathbf{T}_B$) are added to generate the Cauchy stress $\mathbf{T}$, i.e.

$$\mathbf{T} = \mathbf{T}_{\mathrm{C}} = \mathbf{T}_A + \mathbf{T}_B. \tag{2.16}$$

The visco-plastic properties necessary to model the unloading behaviour of the PVC can also be determined from the results of uniaxial tests. The experiments were conducted at strain rates of $\dot{\varepsilon}_0 = 4$ and $\dot{\varepsilon}_0 = 40\%/\,\text{min}$ up to a peak strain of 140%, followed by unloading. The specific material parameters applicable for the PVC are as follows: $q \approx 2.0\,\text{MPa}$; $s \approx 0$; $E_2' \approx 0.5\,\text{MPa}$.

The parameter $\dot{\gamma}_0$ accounts for the influence of strain rates on the mechanical response of untreated PVC. As is evident from (2.9), the strain rate influences are controlled by the material parameter α. In order to determine α, it is necessary to conduct experiments where the PVC membrane material is subjected to a state of inhomogeneous strain. The details of the experimental investigations are given in [30,36] and involve the uniaxial monotonic stretching of a membrane fixed symmetrically along oblique planes. A computational modelling of the experimental configuration can be used to estimate α. Since the elasticity parameters C_1' and C_2' have a logarithmic dependency on the combined stretch rate $\dot{\gamma}_0$ (see e.g. (2.8)), there appears to be only a marginal sensitivity of the computational results to the parameter α. The correlations between the experimental results and computational modelling were performed with different values of the parameters α conducted at axial stretching rates of $\dot{\eta} = 2$ and 20 mm/min. At an extension of $\eta \leqslant 7\,\text{mm}$, which corresponds to a maximum biaxial stretch $\lambda_1 \approx \lambda_2 \approx 1.15$, the computations show only marginal dependence on the value of α. The parameter α has an influence on the computational results only at larger extensions ($\eta > 7\,\text{mm}$) where slip takes place between the metal grips and the PVC specimen leading to unreliable estimates of the load—displacement responses. A comparison between the computational predictions and the experimental results obtained at two extension rates indicate that the parameter $\alpha \approx 3$.

The model parameters obtained were used to predict the behaviour of the untreated PVC subjected to uniaxial stretching at

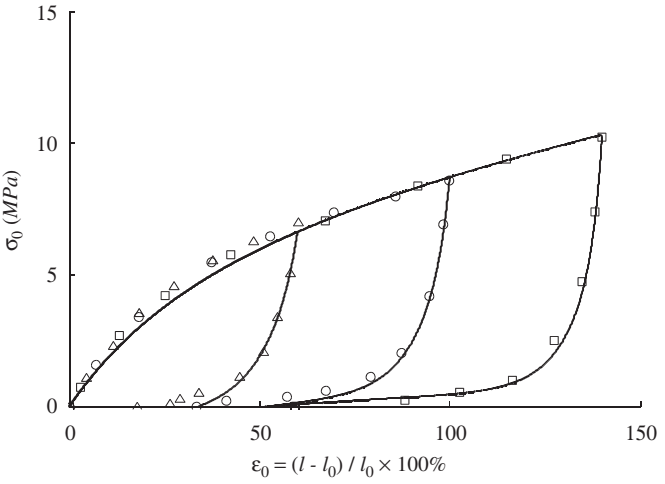

Fig. 3. Uniaxial stress–strain behaviour of an untreated PVC membrane material tested at a strain rate $\dot{\varepsilon}_0 = 160\%/\,\text{min}$. The symbols represent experimental results.

a strain rate of $\dot{\varepsilon}_0 = 160\%/\,\text{min}$. A comparison of experimental results and model predictions is shown in Fig. 3.

2.2. A model for the ethanol-treated PVC

Results of uniaxial tests conducted on the ethanol-treated PVC membrane materials indicate the gradual loss of hyperelasticity as the plasticizer leaches from the specimen (Fig. 1). Therefore, in order to develop a comprehensive model of the progressive evolution of loss of hyperelasticity, it is necessary to incorporate the influences of chemical diffusion on the constitutive responses. The experimental results, however, indicate that beyond a certain duration of exposure to ethanol, the stress–strain relationship for the PVC remains virtually unaltered. Considering this observation, it is feasible to focus on the development of a constitutive model for the chemically treated PVC by considering a threshold duration of a 7-month exposure period. Experimental observations also showed a drastic loss of hyperelasticity as ethanol diffused into the PVC membrane and leached the plasticizer: In terms of the stress–strain response, the hyperelasticity of the untreated material is replaced by a nearly linear elastic response with a pronounced yield point accompanied by both strain softening and strain hardening responses. As the chemically treated PVC deforms it is capable of sustaining appreciable post-yield strains without failure and fracture. The development of a constitutive model for the ethanol-treated PVC can be approached in a variety of ways: for consistency, however, we develop a constitutive model following the basic framework used in developing the constitutive model for the untreated PVC. We select a neo-Hookean form of the internal energy function, which can be derived from an internal energy function with $C_2' \equiv 0$, which reduces to the classical neo-Hookean isotropic model in situations where an infinitesimal strain measure is used. Therefore, for the ethanol-treated PVC, the internal energy function applicable to the loading range associated with the experiments can be written as

$$W^{\mathrm{e}}(I_1^{\mathrm{e}}, I_2^{\mathrm{e}}) = C_1'(I_1^{\mathrm{e}} - 3), \tag{2.17}$$

where

$$C_1' = C_1 + \begin{cases} \kappa_1 \ln(|\dot{\gamma}_0|/\dot{\gamma}_c) & (|\dot{\gamma}_0| \geqslant \dot{\gamma}_c), \\ 0 & (|\dot{\gamma}_0| < \dot{\gamma}_c). \end{cases} \tag{2.18}$$

The results from a series of relaxation tests and uniaxial loading tests conducted at loading rates $\dot{\varepsilon}_0 = 0.4$, 4 and 40%/min are used to determine C_1' [30] and provide the following set of parameters defining the strain rate dependency: $C_1 \approx 14.2\,\text{MPa}$; $\kappa_1 \approx 12.06$; $\dot{\gamma}_c \approx 5.67 \times 10^{-7}\,\text{s}^{-1}$. (We note here that considerable time is required to reach failure; the experimental investigations cited were conducted mainly to examine the linear elastic modulus of the chemically treated material, and the experiments were terminated once yield was observed.) The magnitude of the *rate-independent threshold strain rate* ($\dot{\gamma}_c$) was approximately the same for both the *untreated* and the *ethanol-treated* PVC membrane materials. Furthermore, the departure from elastic behaviour initiates with the yield of the ethanol-treated PVC, with the yield strain roughly corresponding to $\zeta_y \approx 2.8\%$. This suggests that ζ_y is relatively uninfluenced by the duration of chemical exposure. The yield strain thus corresponds to the state resulting from the fracture of the transitional link, which can occur at a critical strain $\varepsilon_0 = \gamma_0 = \zeta_y$. Its dominant presence is then determined from the degree of susceptibility of the transitional link to ethanol exposure. The duration of ethanol exposure, however, has little influence on the elasticity characteristics of the elastic recovery model *A*. Changes in the elasticity characteristics of the recovery model *A* will be influenced by the breakage of the transitional links. Following the modelling adopted for the untreated PVC, the elastic parameter E_2' is considered to be a constant. The parameter E_1', however, takes into consideration material yield and can be represented in the form

$$E_1' = \begin{cases} \to \infty & (\dot{\gamma}_0 \geqslant -\dot{\gamma}_c^v \text{ and } \gamma_0 \leqslant \zeta_y), \\ E_y' & (\dot{\gamma}_0 \geqslant -\dot{\gamma}_c^v \text{ and } \gamma_0 > \zeta_y), \\ 0 & (\dot{\gamma}_0 < -\dot{\gamma}_c^v). \end{cases} \tag{2.19}$$

In (2.19), ζ_y is the yield strain and E_y' can be interpreted as the post-yield *hardening modulus*. This particular representation of E_1' takes into consideration the complete elastic behaviour of the treated material before yield at a loading rate $\dot{\gamma}_0 \geqslant -\dot{\gamma}_c^v$, where the visco-plastic deformation is restricted by the value of infinity assigned to E_1'. Beyond the yield point, E_1' has a finite value. This, however, results in the development of visco-plastic deformations, contributing to the initial softening and subsequent hardening behaviour, particularly in the large strain range (e.g. $\varepsilon_0 = 100$–150%). During unloading (i.e. $\dot{\gamma}_0 < -\dot{\gamma}_c^v$), visco-plastic effects are fully activated due to the fact that $E_1' = 0$, and this contributes to significant irreversible visco-plastic strains. We also consider the possible influences of the rate-dependency on the *hardening modulus* E_y', which is modelled according to the relationship

$$E_y' = E_y + \begin{cases} \kappa_y \ln(\dot{\gamma}_0/\dot{\gamma}_c^v) & (\dot{\gamma}_0 \geqslant \dot{\gamma}_c^v), \\ 0 & (-\dot{\gamma}_c^v \leqslant \dot{\gamma}_0 < \dot{\gamma}_c^v), \end{cases} \tag{2.20}$$

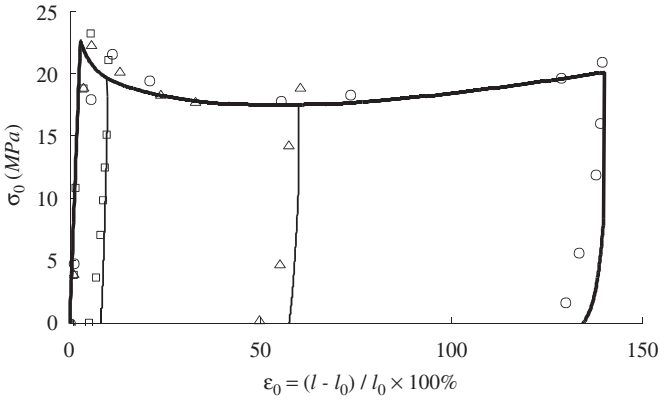

Fig. 4. Uniaxial stress–strain behaviour of a chemically treated PVC membrane material tested at a strain rate $\dot{\varepsilon}_0 = 160\%/\,\text{min}$. The symbols represent experimental results.

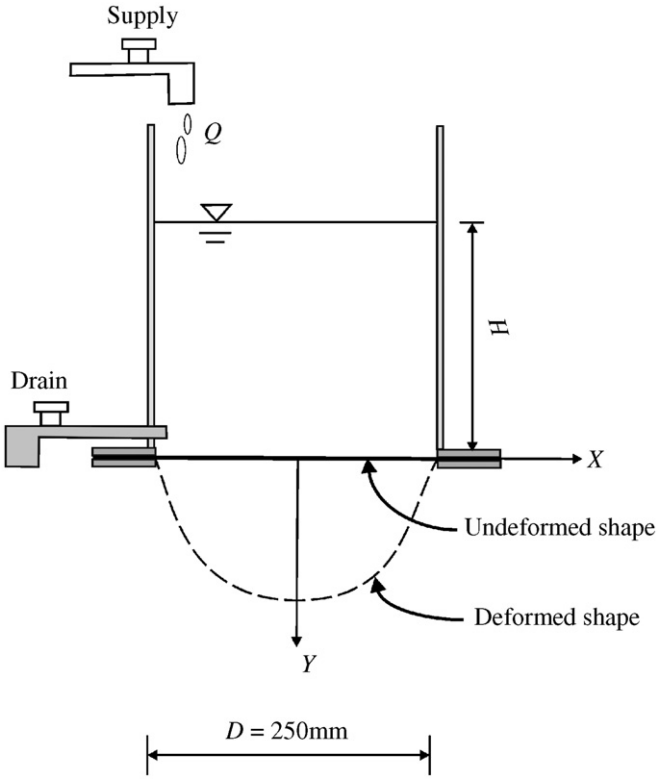

Fig. 5. Fluid pressure loading of a PVC membrane fixed along a circular boundary.

where κ_y is the rate-sensitivity and E_y is the *rate-independent hardening modulus*. To account for the visco-plastic responses in the ethanol-treated PVC, we adopt the form of (2.15). In contrast to the untreated PVC material, the visco-plastic response dominates the unloading mode, and beyond the yield point ζ_y, also takes into consideration the softening response.

In the parameter identification exercise we first examine the time-independent behaviour of the PVC. In the ethanol-treated PVC, there is a noticeable yield point associated with the proposed time-independent stress–strain response. The absence of softening suggests the applicability of the assumption concerning the absence of a viscous effect at limiting loading rates less than $\dot{\gamma}_c^v$. We can determine the *static yield stress* $q(=6C_1\zeta_y) \approx 2.4\,\text{MPa}$ from the time-independent stress–strain curve. The parameters E_y and E_2' can be determined by matching the *slope* of the hardening response of the time-independent stress–strain curve; using this procedure we obtain $E_y \approx 1.1\,\text{MPa}$ and $E_2' \approx 1.2\,\text{MPa}$. The parameter E_y' that accounts for the rate-dependency can be obtained by matching the slope of the hardening responses for a set of loading tests conducted at the loading rates $\dot{\varepsilon}_0 = 4$ and 40%/min. Considering such a procedure, the constitutive parameters required to characterize the ethanol-treated PVC are obtained as follows: $E_y \approx 1.13\,\text{MPa}$; $\kappa_y \approx 0.13$; $\dot{\gamma}_c^v \approx 3.2 \times 10^{-10}\,\text{s}^{-1}$. The viscous sensitivity s is the only remaining parameter introduced in (2.15). As $s \to 0$, the unloading behaviour of the material (with $E_1' = 0$) is virtually uninfluenced by the loading rate. Considering the softening region, where $E_1' \neq \infty$, the rate-sensitivity is appreciable even though s approaches zero. The value of s therefore has a significant influence on the softening response of the material, since, beyond the yield point, E_1' transforms abruptly from an infinite value to a finite value (i.e. $\varepsilon_0 = \zeta_y$). The parameter identification exercises performed on the stress–strain curves derived at loading rates $\dot{\varepsilon}_0 = 4$ and 40%/min indicate that $s \approx 0.1$. The visco-plastic behaviour of the chemically treated PVC can be defined by the parameters: $q \approx 2.4\,\text{MPa}$; $s \approx 0.1$; $\dot{\gamma}_c^v \approx 3.2 \times 10^{-10}\,\text{s}^{-1}$. The results for the time-independent response and the stress–strain curves derived up to failure at loading rates of $\dot{\varepsilon}_0 = 4$ and 40%/min by material parameters indicate that accurate representations are obtained for the yield behaviour of the material, followed by a material softening and a moderate amount of hardening at large deformations (i.e. strains in the range $\varepsilon_0 = 100$–150%). The material parameters were further used to evaluate the computational responses of a test specimen fixed along oblique directions and subjected to an axial extension rate of $\dot{\eta} = 2\,\text{mm}/\,\text{min}$. The computational evaluations were performed with different values of the parameter α. Since the plasticizer loss appears to stabilize after 5 *months* of exposure [50], it may be concluded that the material parameter α is virtually uninfluenced by the duration of chemical exposure. Considering the discussion pertaining to the evaluation of the parameter α for the untreated material, it could be concluded that the value $\alpha \approx 3$ is also applicable to the PVC membrane material when exposed to ethanol for a period of 7 months. This value is possibly indicative of equal contributions from the three principal stretch directions of the polymeric material in the definition of $\dot{\gamma}_0$ in (2.19). The model parameters for the ethanol-treated PVC membrane material developed using experimental data from tests conducted at strain rates of $\dot{\varepsilon}_0 = 4$ and 40%/min were used to predict the response that would be obtained for a ethanol-treated PVC material uniaxial test conducted at a strain rate of $\dot{\varepsilon}_0 = 160\%/\,\text{min}$. The comparison between experimental results and computational predictions are shown in Fig. 4.

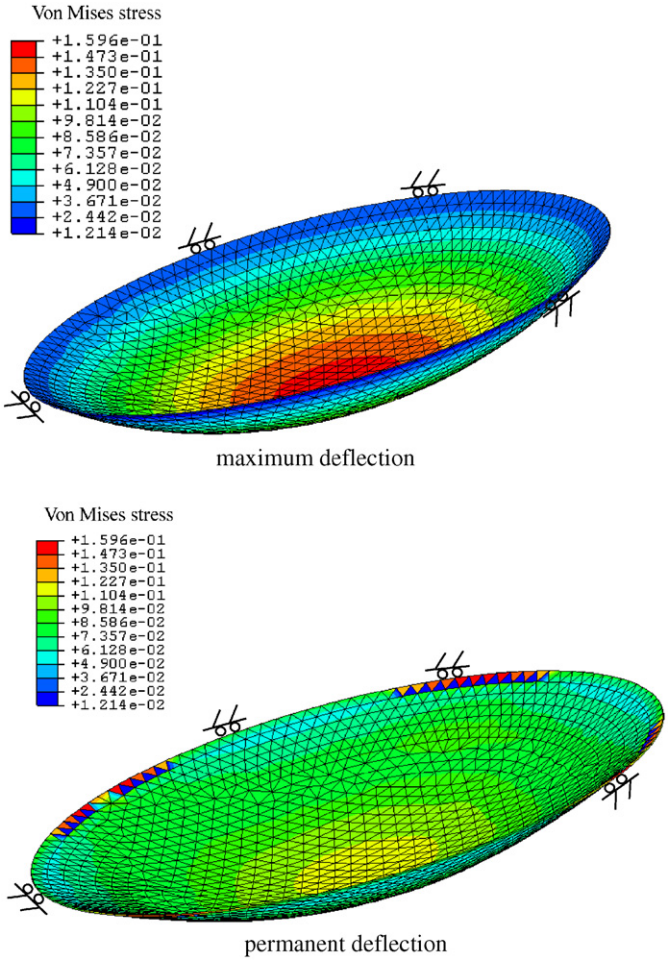

Fig. 6. Hydraulic loading on an untreated circular membrane. Total number of elements: 2402; maximum fluid pressure corresponds to 1 m of water.

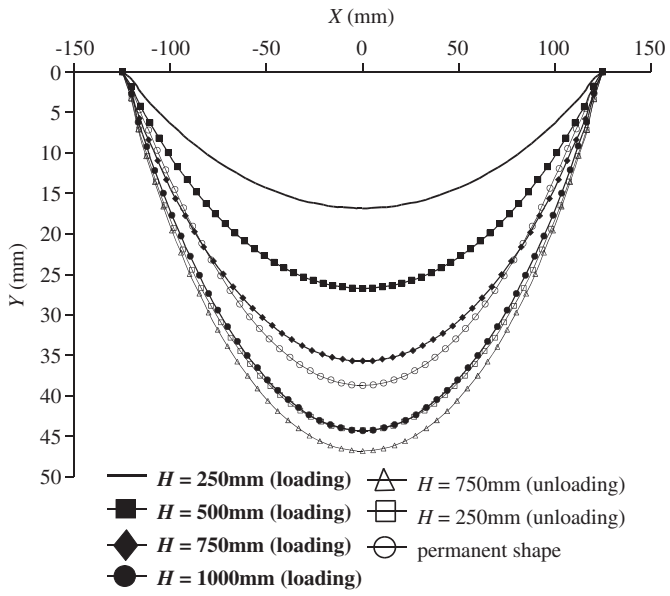

Fig. 7. The deflected shape of the untreated circular membrane under the action of fluid accumulation in the reservoir. Maximum fluid pressure corresponds to 1 m of water.

3. Mechanics of PVC membranes

PVC membranes are used as engineered barriers; it is therefore instructive to apply the constitutive models presented previously to examine the mechanics of membranes, both untreated and ethanol-treated, to investigate the behaviour of typical membrane configurations. The forms of the constitutive models presented in the previous section are such that analytical solutions for even the simplest axisymmetric problems cannot be obtained conveniently. Consequently, a computational approach is adopted to examine a range of problems of engineering interest. The specific problems that are examined here include the application of fluid pressures to edge-supported membranes with circular, square and triangular planforms. An additional problem considers the fluid pressure-induced deflection of an edge-supported untreated circular PVC membrane containing a circular patch that has been subjected to chemical exposure. These computations were performed using the general-purpose finite element code ABAQUS (ABAQUS/Standard [51]). There are several computational features in ABAQUS/Standard relevant to the computational modelling of the axisymmetric/asymmetric membrane loading

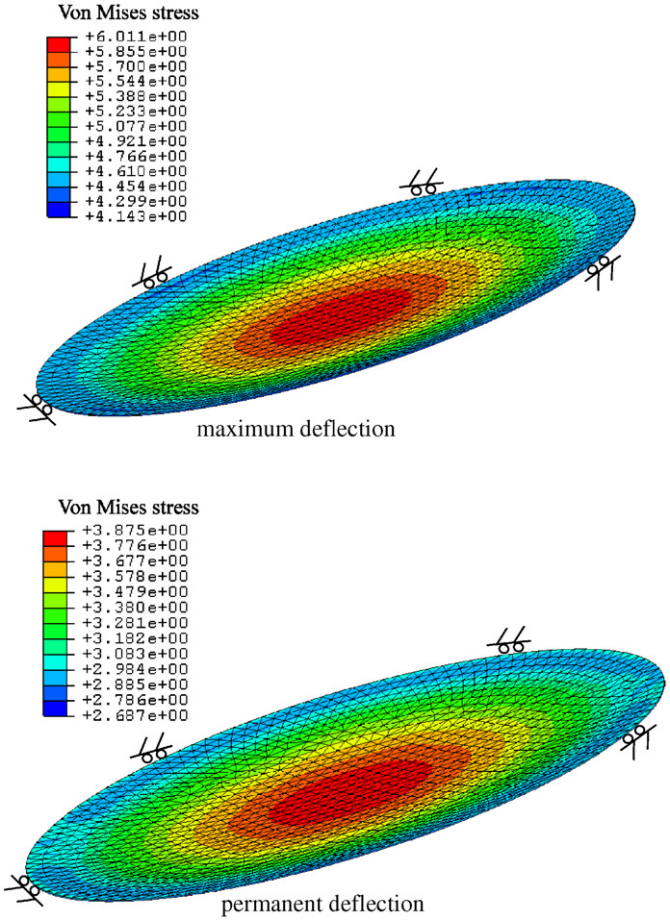

Fig. 8. Hydraulic loading on a chemically treated circular membrane. Total number of elements: 2402; maximum fluid pressure corresponds to 1 m of water.

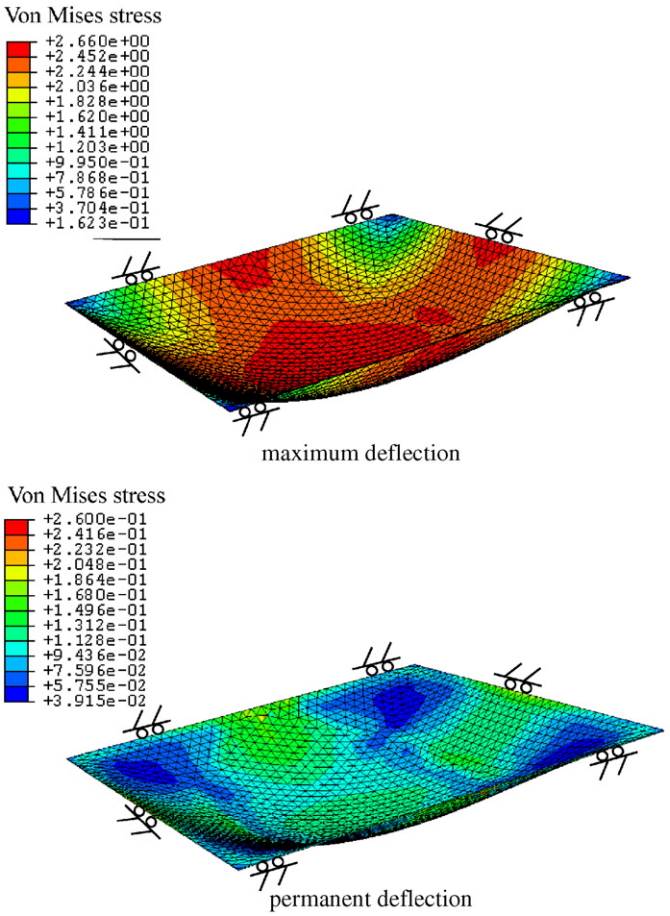

Fig. 9. Hydraulic loading on an untreated square membrane. Total number of elements: 2998; maximum fluid pressure corresponds to 1 m of water.

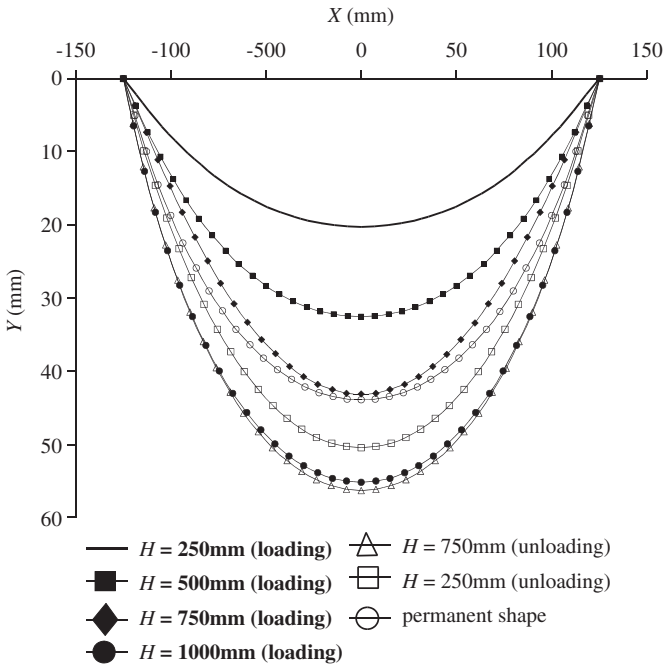

Fig. 10. The deflected shape of the untreated square membrane under the action of fluid accumulation in the reservoir. Maximum fluid pressure corresponds to 1 m of water.

problems and include consideration of large strain phenomena, and, most importantly, the ability to implement the constitutive model derived in Section 2 in the computational algorithm. Complete descriptions of these procedures are contained in the supplied document in ABAQUS/Standard, which is discussed in the User Subroutine UMAT (ABAQUS/Standard [51]). In this study, only the last feature will be discussed. In the nonlinear analysis using the ABAQUS/Standard code, each step is divided into iteration increments. In this analysis, we chose the size of the first loading increment, and the ABAQUS/Standard code automatically assigns the size of subsequent increments. During each increment, the code employs a Newton–Raphson algorithm to perform the iterations and the equilibrium is determined through consideration of the principle of virtual work, i.e.

$$\int_{V^{\langle t+\Delta t\rangle}} \mathbf{T}^{\langle t+\mathrm{d}t\rangle} : \delta\mathbf{D}^{\langle t+\mathrm{d}t\rangle}\,\mathrm{d}V^{\langle t+\mathrm{d}t\rangle} = \int_{S^{\langle t+\Delta t\rangle}} \mathbf{t}^{\langle t+\mathrm{d}t\rangle} \bullet \delta\mathbf{v}\,\mathrm{d}S^{\langle t+\mathrm{d}t\rangle} + \int_{V^{\langle t+\Delta t\rangle}} \mathbf{f}^{\langle t+\mathrm{d}t\rangle} \bullet \delta\mathbf{v}\,\mathrm{d}V^{\langle t+\mathrm{d}t\rangle}, \tag{3.1}$$

where $\mathbf{T}$ is the Cauchy stress, $\delta\mathbf{D}$ is the incremental strain rate, $\delta\mathbf{v}$ is a vector of virtual displacements, $\mathbf{t}$ is a vector of externally applied surface tractions on a unit surface of S, $\mathbf{f}$ is a body force vector on a unit volume of V and $^{\langle t+\mathrm{d}t\rangle}$ denotes a state evaluated at time $t+\mathrm{d}t$. For the Newton–Raphson algorithm, we require the Jacobian of the finite element equilibrium equations. The Jacobian, which is obtained by taking the variation of Eq. (3.1), can be written as

$$\int_{V^{\langle t+\mathrm{d}t\rangle}} (\mathrm{d}\mathbf{T}^{\langle t+\mathrm{d}t\rangle} : \delta\mathbf{D}^{\langle t+\mathrm{d}t\rangle} + \mathbf{T}^{\langle t+\mathrm{d}t\rangle} : \mathrm{d}\delta\mathbf{D}^{\langle t+\mathrm{d}t\rangle})\,\mathrm{d}V^{\langle t+\mathrm{d}t\rangle} = \int_{S^{\langle t+\mathrm{d}t\rangle}} \left(\mathrm{d}\mathbf{t}^{\langle t+\mathrm{d}t\rangle} \bullet \delta\mathbf{v} + \mathbf{t}^{\langle t+\mathrm{d}t\rangle} \bullet \delta\mathbf{v}\frac{\mathrm{d}A}{A}\right)\mathrm{d}S^{\langle t+\mathrm{d}t\rangle} + \int_{V^{\langle t+\mathrm{d}t\rangle}} \left(\mathrm{d}\mathbf{f}^{\langle t+\mathrm{d}t\rangle} \bullet \delta\mathbf{v} + \mathbf{f}^{\langle t+\mathrm{d}t\rangle} \bullet \delta\mathbf{v}\frac{\mathrm{d}J}{J}\right)\mathrm{d}V^{\langle t+\mathrm{d}t\rangle} \tag{3.2}$$

with

$$A = \frac{\mathrm{d}S^{\langle t+\mathrm{d}t\rangle}}{\mathrm{d}S^{\langle t\rangle}}, \quad J = \frac{\mathrm{d}V^{\langle t+\mathrm{d}t\rangle}}{\mathrm{d}V^{\langle t\rangle}}, \tag{3.3}$$

where A is the surface area ratio between time $t+\mathrm{d}t$ and t, and J is the volume ratio between time $t+\mathrm{d}t$ and t. The right side of Eq. (3.2) is defined by the boundary conditions involving the loading conditions and displacement constraints. On the left side, the expressions for the strain measure $\mathbf{D}$ and its variations $\mathrm{d}\mathbf{D}$ and $\mathrm{d}\delta\mathbf{D}$ in terms of the virtual displacement are defined by the displacement interpolation function used in the element definition. It has been shown (ABAQUS/Standard [51]) that the

left side of Eq. (3.2) can be expressed in a more explicit form:

$$\int_{V^{\langle t+\mathrm{d}t\rangle}} \left\{ \mathrm{d}\mathbf{D}^{\langle t+\mathrm{d}t\rangle} : \mathbf{C}^{\langle t+\mathrm{d}t\rangle} : \delta\mathbf{D}^{\langle t+\mathrm{d}t\rangle} - \frac{1}{2}\mathbf{T}^{\langle t+\mathrm{d}t\rangle} : [2\mathbf{D}^{\langle t+\mathrm{d}t\rangle} \bullet \mathbf{D}^{\langle t+\mathrm{d}t\rangle} - (\mathbf{L}^{t+\mathrm{d}t})^{T} \bullet \mathbf{L}^{t+\mathrm{d}t}] \right\} \mathrm{d}V^{\langle t+\mathrm{d}t\rangle},$$

where $\mathbf{C}$ is the tangential stiffness and a fourth-order tensor defined by

$$\mathbf{C} = \frac{\partial(\mathrm{d}\mathbf{T})}{\partial(\mathrm{d}\mathbf{D})}. \tag{3.4}$$

The data on both $\mathbf{C}$ and $\mathbf{T}$ are defined by the constitutive responses of the PVC material implemented through the subroutine UMAT available in the ABAQUS/Standard code. The ABAQUS/Standard further utilizes a backward-Euler scheme as a default finite difference scheme to update variables. Those variables that are determined from previous iterations and do not change during the iteration between $[t, t + \mathrm{d}t]$ can be defined as *state variables*. The *state variables* adopted in this analysis include the components of the irreversible deformation gradient $\mathbf{F}^{u}$ at time t and the stress tensors at time t, in the visco-plastic component including models A and B. When a fully backward-Euler finite difference scheme in time is implemented, the updating of $\dot{\gamma}_0$ requires information on the material configuration at $t + \mathrm{d}t$. The updated value of $\dot{\gamma}_0$ will have a direct influence on the elasticity parameters for the element C in the chosen constitutive model, with the result that the computations will exhibit non-convergence. The value of $\dot{\gamma}_0$ is thus assumed to remain unchanged during iteration and is taken as a further *state variable*. For the problems examined here, the PVC membrane only experiences incremental loading during the initial stage where irreversible deformations are absent; the initial values of the state variables can therefore be obtained by treating the material as fully elastic. The state variables are updated only when the iteration converges. Both a quadratic triangular membrane element (3M6) and a linear solid triangular prism element (C3D6) were utilized in the computational modelling. The results indicated no noticeable differences between the two types of elements. The computations presented in the paper were developed using the solid triangular prism element.

3.1. Uniform loading of an edge-supported circular membrane

In this example we consider the fluid loading of a circular PVC membrane of radius 125 mm, which is fixed at the boundary (Fig. 5). The membrane is loaded by fluid (water at a density of ρ=1 g/cc) pressures that are applied through accumulation of fluid in a reservoir at a prescribed rate $Q = 12\,\mathrm{L/min}$. Since the membrane deflects a substantial amount during the application of the fluid loading, the applied fluid pressure is non-uniform with an axisymmetric variation roughly corresponding to the height of the fluid in the reservoir. The maximum fluid pressure applied to the membrane corresponds to 1 m of water. This is a departure from the usual uniform air-pressurization approximation used in the testing of membranes but the example represents a useful model of a condition that can be encountered in practice. The unloading is carried out by the removal of the fluid at the same emptying rate. The computational modelling uses the finite element discretization of the circular membrane region shown in Fig. 6. Fig. 7 shows the deflected shape of the untreated PVC circular membrane for various levels of fluid accumulation and fluid withdrawal. Analogous results for the case involving the ethanol-treated PVC circular membrane are shown in Fig. 8. It may be noted that the computational modelling illustrates the development of permanent deformations in both untreated and chemically treated membranes during the loading–unloading process.

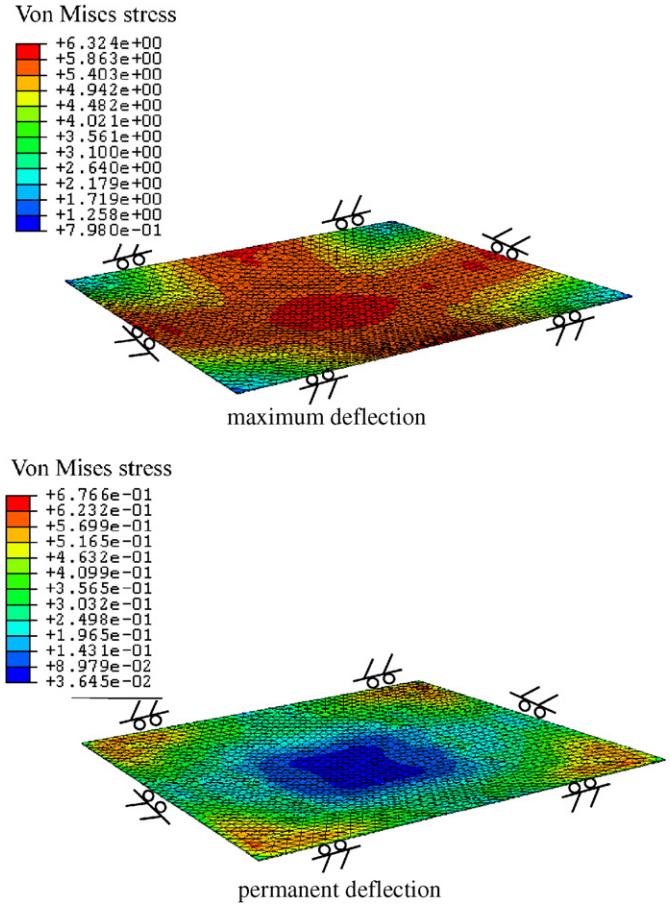

Fig. 11. Hydraulic loading on chemically treated square membrane. Total number of elements: 2998; maximum fluid pressure corresponds to 1 m of water.

3.2. Uniform loading of an edge-supported square membrane

In the second example we consider the problem of a square PVC membrane that is fixed at the boundary and subjected to fluid loading similar to that described in Section 3.1. The finite element model of the membrane region is shown in Fig. 9. The deflected shapes of the square membrane along one of the axes of symmetry, for both loading and unloading paths and for both the treated and untreated PVC membranes are shown in

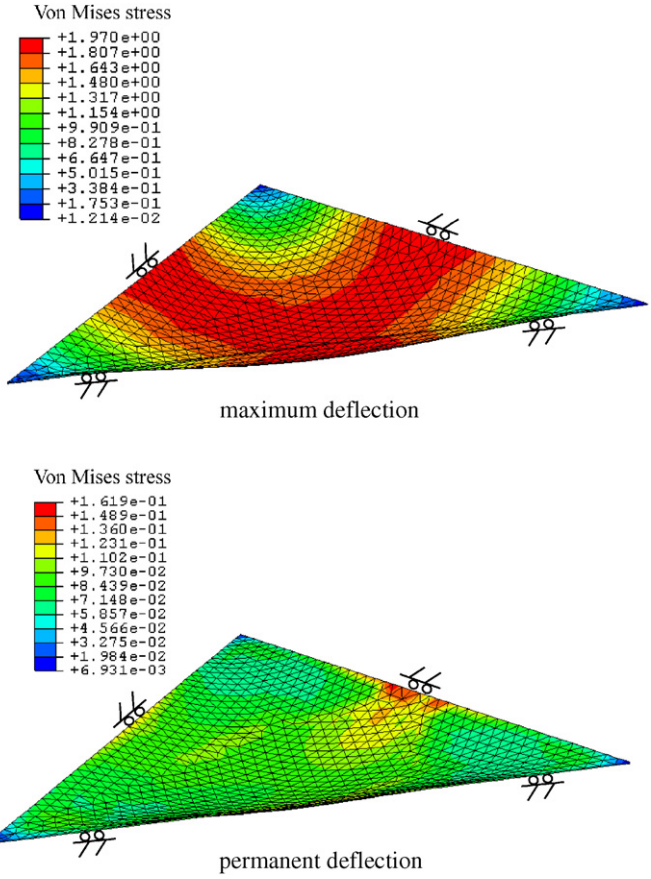

Fig. 12. Hydraulic loading on an untreated equilateral triangular membrane. Total number of elements: 1712; maximum fluid pressure corresponds to 1 m of water.

Fig. 10. The maximum fluid pressure applied to the membrane corresponds to 1 m of water. The deflection of the chemically treated PVC is significantly lower (see Fig. 11). The results for the deflection of the membrane during the loading–unloading process display characteristics similar to those observed in connection with the fluid loading of the untreated and chemically treated circular membrane.

3.3. Uniform loading of an edge-supported equilateral triangular membrane

In the third example we examine the deflection of an equilateral triangular membrane that is fixed at the boundary and subjected to fluid loading similar to that described previously. The finite element model of the membrane region is shown in Fig. 12. The deflected shapes of the untreated equilateral membrane, along an axis of symmetry, for both loading and unloading paths are shown in Fig. 13. The deflection of the chemically treated PVC is limited (see Fig. 14). The results for the deflection of the membrane during the loading–unloading process display characteristics similar to those observed in connection with the fluid loading of the untreated and chemically treated circular and square membranes.

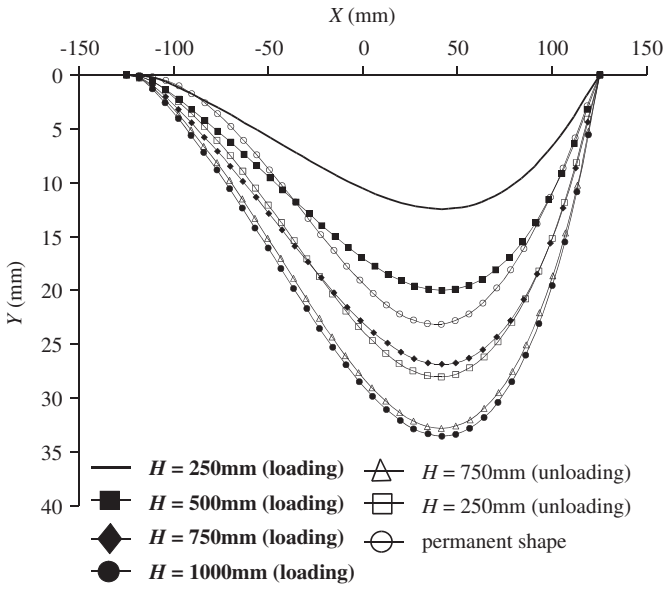

Fig. 13. The deflected shape of the untreated equilateral triangular membrane under the action of fluid accumulation in the reservoir. Maximum fluid pressure corresponds to 1 m of water.

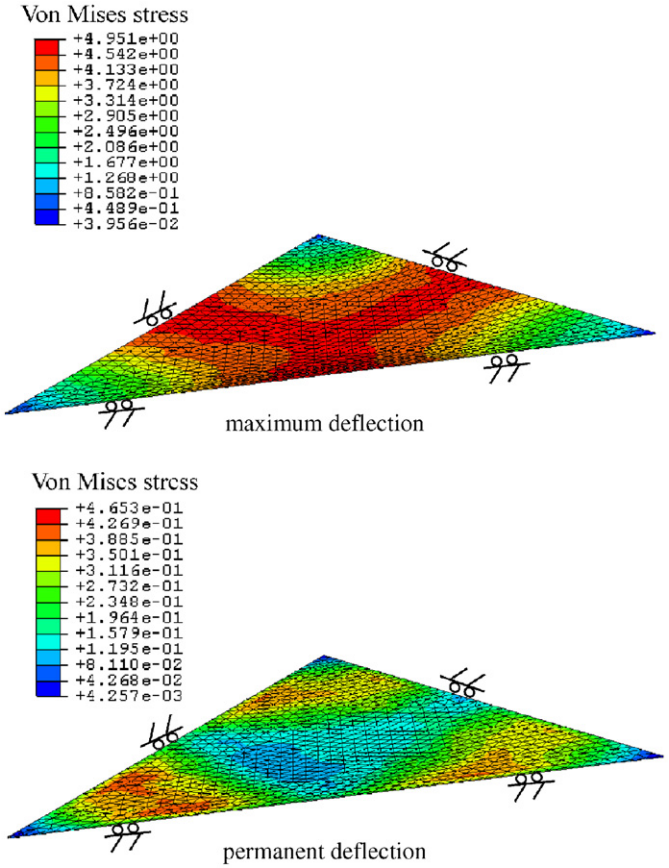

Fig. 14. Hydraulic loading on a chemically treated equilateral triangular membrane. Total number of elements: 1712; maximum fluid pressure corresponds to 1 m of water.

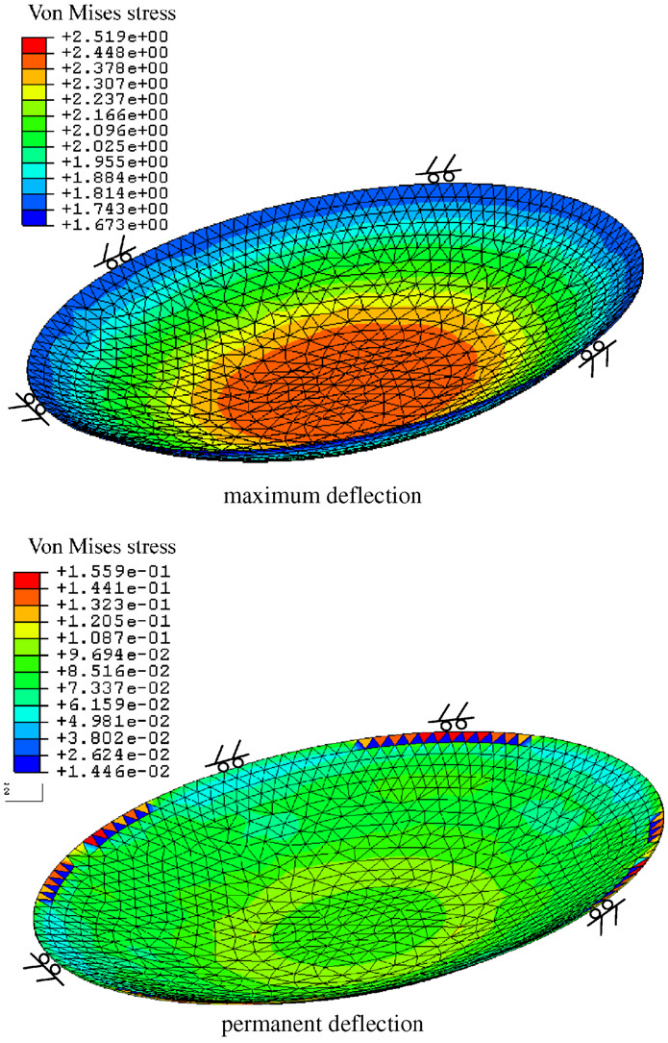

Fig. 15. Hydraulic loading on an untreated circular membrane with a central circular patch. Total number of elements: 3770; maximum fluid pressure corresponds to 1 m of water; ratio between diameter of patch and that of the membrane: 0.32.

3.4. Fluid pressure loading of a membrane containing a circular patch subjected to chemical exposure

In this section we examine the problem of the fluid pressure loading of a PVC membrane that contains a circular patch that has been subjected to chemical exposure. The ratio between the diameter of the patch and that of the membrane is 0.32. The geometry of the problem is shown in Fig. 15. The maximum fluid height applied to the membrane is 1 m. Fig. 16 shows the deflected shape of the untreated PVC circular membrane for various levels of the fluid accumulation and fluid withdrawal. The central patch zone deflects as a rigid region and this contributes to a reduction in the overall deflections and the corresponding permanent deflections. The junction between the two regions invariably exhibits sharp changes in the curvature, which can be a source for concern, especially with regard to the development of fracture and damage at those locations.

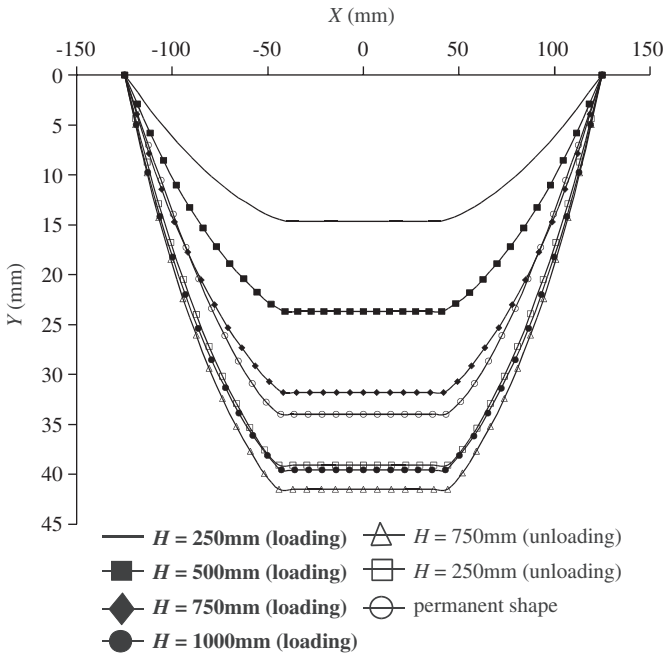

Fig. 16. The deflected shapes of the untreated circular membrane with a central circular patch under the action of fluid accumulation in the reservoir. Ratio between diameter of patch and that of the membrane: 0.32; maximum fluid pressure corresponds to 1 m of water.

4. Concluding remarks

The use of PVC membranes as liners or engineered barriers for landfill implicitly assumes that the hyperelastic attributes of the liners remain unaltered throughout the lifetime of the barrier. Experimental research points to the loss of hyperelasticity that can result from direct contact of the PVC with chemicals such as acetone and ethanol. The chemical leaching of plasticizer from the PVC also results in a barrier material that exhibits distinct yield-like stress–strain characteristics. It is shown that the mechanical behaviour of the untreated PVC can be modelled as a rate-sensitive hyperelastic material with internal energy functions that are loading path-dependent. The ethanol-treated PVC can also be modelled using the general approach developed to describe the constitutive behaviour of the untreated PVC. The material parameters required to describe both responses can be experimentally determined and the constitutive models themselves are amenable for implementation in general-purpose finite element computational schemes that accommodate hyperelasticity and strain rate sensitivity. The computational schemes are used to examine the mechanics of edge-supported PVC membranes that are subjected to loading by fluid pressure. The computational results show trends that are consistent with those obtained from experiments involving transverse indentation of both untreated and treated edge-supported PVC membranes by fluid pressure. The problems examined provide further experimental arrangements for examining the validity of the constitutive models and their computational implementations.

Acknowledgements

The work described in the paper was supported through a *Discovery Grant* awarded by the Natural Sciences and Engineering Research Council of Canada awarded to the first author, who would also like to acknowledge the research support received by the Max Planck Gesellschaft through the Award of the *2003 Max Planck Forschungspreis in the Engineering Sciences*. Both authors are grateful for the assistance of Stanford University towards to development of the computational solutions.

References

[1] G.I. Barenblatt, D.D. Joseph (Eds.), Collected Papers of R.S. Rivlin, vols. I, II, Springer, Berlin, 1997.
[2] A.E. Green, J.E. Adkins, Large Elastic Deformations, Oxford University Press, London, 1970.
[3] L.R.G. Treloar, Rubber Elasticity, third ed., Oxford University Press, London, 1975.
[4] L.R.G. Treloar, The mechanics of rubber elasticity, Proc. R. Soc. Ser. A 351 (1976) 301–330.
[5] C. Truesdell, W. Noll, The Non-Linear Field Theories of Mechanics, second ed., Springer, Berlin, 1992.
[6] R.T. Deam, S.F. Edwards, The theory of rubber elasticity, Philos. Trans. R. Soc. 280 (1976) 317–353.
[7] R.W. Ogden, Non-Linear Elastic Deformations, Ellis-Horwood, Chichester, 1984.
[8] A.I. Lur'e, Nonlinear Theory of Elasticity, North-Holland, Amsterdam, 1990.
[9] A.D. Drozdov, Finite Elasticity and Viscoelasticity, World Scientific, Singapore, 1996.
[10] A. Dorfmann, A. Muhr (Eds.), Constitutive Models for Rubber, A.A. Balkema, Rotterdam, 1999.
[11] M.C. Boyce, E.M. Arruda, Constitutive models of rubber elasticity, a review, Rubber Chem. Technol. 73 (3) (2000) 504–523.
[12] in: Y.B. Fu, R.W. Ogden (Eds.), Nonlinear Elasticity: Theory and Applications, Cambridge University Press, Cambridge, 2001.
[13] D. Besdo, R.H. Schuster, J. Ihlemann (Eds.), Constitutive Models for Rubber II, in: Proceedings of the 2nd European Conference on Constitutive Models for Rubber, Hanover, Germany, A.A. Balkema, Lisse, 2001.
[14] J.J.C. Busfield, A.H. Muhr (Eds.), Constitutive Models for Rubber III, in: Proceedings of the 3rd European Conference on Constitutive Models for Rubber, London, UK, A.A. Balkema, Lisse, 2003.
[15] G. Saccomandi, R.W. Ogden (Eds.), Thermomechanics of Rubber-like Materials, in: CISM Lecture Notes, vol. 452, Springer, Wien, 2004.
[16] A.P.S. Selvadurai, Second-order elasticity for axisymmetric torsion, in: E. Croitoro (Ed.), Proceedings of the 2nd Canadian Conference on Nonlinear Solid Mechanics, Vancouver, vol. 1, 2002, pp. 27–49.
[17] R.S. Rivlin, The relation between the Valanis–Landel and classical strain energy functions, Int. J. Non-Linear Mech. (2006) 141–145.
[18] A.P.S. Selvadurai, Deflections of a rubber membrane, J. Mech. Phys. Solids 54 (2006) 1093–1119.
[19] E.M. Arruda, M.C. Boyce, R. Jayachandran, Effects of strain rate, temperature and thermo-mechanical coupling on the finite strain deformation of glassy polymers, Mech. Mater. 19 (1995) 193–212.
[20] J. Sweeney, I.M. Ward, Rate dependent and network phenomena in the multi-axial drawing of poly(vinyl chloride), Polymer 36 (2) (1995) 299–308.
[21] M.C. Boyce, D.M. Parks, A.S. Argon, Large inelastic deformation of glassy polymers, part I: rate dependent constitutive model, Mech. Mater. 7 (1988) 15–33.
[22] A.S. Wineman, K.R. Rajagopal, On a constitutive theory for materials undergoing microstructural changes, Arch. Mech. 42 (1990) 53–74.
[23] K.R. Rajagopal, A.S. Wineman, A constitutive equation for non-linear solids which undergo deformation induced microstructural changes, Int. J. Plasticity 83 (1992) 385–395.
[24] J.S. Bergström, M.C. Boyce, Constitutive modelling of the large strain time- dependent behaviour of elastomers, J. Mech. Phys. Solids 46 (5) (1998) 931–954.
[25] E.G. Septanika, L.J. Ernst, Application of the network alteration theory for modeling the time-dependent constitutive behaviour of rubbers. Part I. General theory, Mech. Mater. 30 (1998) 253–263.
[26] E.G. Septanika, L.J. Ernst, Application of the network alteration theory for modeling the time-dependent constitutive behaviour of rubbers. Part II. Further evaluation of the general theory and experimental verification, Mech. Mater. 30 (1998) 265–273.
[27] A. Makradi, S. Ahzi, R.V. Gregory, D.D. Edie, A two-phase self-consistent model for the deformation and phase transformation behavior of polymers above the glass transition temperature: application to PET, Int. J. Plasticity 21 (2005) 741–758.
[28] A.F.M.S. Amin, M.S. Alam, Y. Okui, An improved hyperelasticity relation in modeling viscoelasticity response of natural and high damping rubbers in compression: experiments, parameter identification and numerical verification, Mech. Mater. 34 (2002) 75–95.
[29] M.E. Gurtin, L. Anand, The decomposition $\mathbf{F} = \mathbf{F}^{\mathrm{e}}\mathbf{F}^{p}$, material symmetry, plastic irrotationality for solids that are isotropic-viscoplastic or amorphous, Int. J. Plasticity 21 (2005) 1686–1719.
[30] A.P.S. Selvadurai, Q. Yu, Constitutive modelling of a polymeric material subjected to chemical exposure, Int. J. Plasticity 22 (2006) 1089–1122.
[31] J.A. Shaw, A.S. Jones, A.S. Wineman, Chemorheological response of elastomers at elevated temperatures: Experiments and simulations, J. Mech. Phys. Solids 53 (2005) 2758–2793.
[32] R.W. Ogden, D.G. Roxburgh, A pseudoelastic model for the Mullins effect in filled rubber, Proc. Roy. Soc. Ser. A 455 (1999) 2861–2877.
[33] R.W. Ogden, D.G. Roxburgh, An energy-based model of the Mullins effect, in: A. Dorfmann, A. Muhr (Eds.), Proceedings of the 1st European Conference on Constitutive Models for Rubber, Vienna, A.A. Balkema, Rotterdam, 1999, pp. 23–28.
[34] A. Dorfmann, R.W. Ogden, A pseudo-elastic model for loading, partial loading and reloading of particle-reinforced rubber, Int. J. Solids Struct. 40 (2003) 2699–2714.
[35] A. Dorfmann, R.W. Ogden, A constitutive model for the Mullins effect with permanent set in particle-reinforced rubber, Int. J. Solids Struct. 41 (2004) 1855–1878.
[36] Q. Yu, A.P.S. Selvadurai, Mechanical behaviour of a plasticized PVC subjected to ethanol exposure, Polym. Degradation Stab. 89 (2005) 109–124.
[37] E. Kröner, Allgemeine kontinuumstheorie der versetzungen und eigenspannungen, Arch. Ration. Mech. Anal. 4 (1960) 273–334.
[38] E.H. Lee, Elastic-plastic deformation at finite strains, J. Appl. Mech. 36 (1969) 1–6.
[39] A.C. Pipkin, R.S. Rivlin, Mechanics of rate-independent materials, J. Appl. Math. Phys. (ZAMP) 16 (1970) 313–327.
[40] D.R. Owen, A mechanical theory of materials with elastic range, Arch. Ration. Mech. Anal. 37 (1970) 85–110.
[41] R.J. Clifton, On the equivalence of $\mathbf{F}^{\mathrm{e}}\mathbf{F}^{p}$ and $\mathbf{F}^{p}\mathbf{F}^{\mathrm{e}}$, J. Appl. Mech. Trans. ASME 39 (1972) 287–289.
[42] C. Miehe, On the representation of Prandtl–Reuss tensors within the framework of multiplicative elasto-plasticity, Int. J. Plasticity 10 (1994) 609–621.
[43] V.A. Lubarda, Constitutive theories based on the multiplicative decomposition of deformation gradient: thermo-elasticity, elasto-plasticity, and biomechanics, Appl. Mech. Rev. 57 (2004) 95–108.
[44] L.E. Malvern, Introduction to the Mechanics of a Continuous Medium, Prentice-Hall, Upper Saddle River, 1969.
[45] A.J.M. Spencer, Continuum Mechanics, second ed., Dover Publications, London, 2004.
[46] M. Mooney, A theory of large elastic deformation, J. Appl. Phys. 11 (1940) 583–593.
[47] R.S. Rivlin, Large elastic deformations of isotropic materials. IV. Further developments of the general theory, Philos. Trans. R. Soc. A 241 (1948) 379–397.

[48] A.P.S. Selvadurai, Q. Yu, On the indentation of a polymeric membrane, Proc. R. Soc. Math. Phys. Sci. Ser. A 462 (2006) 189–209.
[49] E.M. Arruda, M.C. Boyce, H. Quintus-Bosz, Effects of initial anisotropy on the finite strain deformation behavior of glassy polymers, Int. J. Plasticity 9 (1993) 783–811.
[50] Q. Yu, The Mechanical behaviour of chemically treated PVC geosynthetic membranes, Ph.D. Thesis, McGill University, Montreal, Que., Canada, 2005.
[51] ABAQUS/Standard, A General-Purpose Finite Element Program, Hibbitt, Karlsson & Sorensen, Inc., Pawtucket, RI, 2004.